

# Coupled effects of chemical environments and freeze–thaw cycles on damage characteristics of red sandstone

Feng Gao<sup>1</sup> · Qiaoli Wang<sup>1</sup> · Hongwei Deng<sup>1</sup> · Jian Zhang<sup>1</sup> · Weigang Tian<sup>2</sup> · Bo Ke<sup>1</sup>

Received: 8 March 2016 / Accepted: 28 May 2016 / Published online: 16 June 2016  
© Springer-Verlag Berlin Heidelberg 2016

**Abstract** To study the influence of freeze–thaw cycles under complex chemical environments on the red sandstone, nuclear magnetic resonance (NMR) technology was used to analyze the damage evolution law of red sandstone. The freeze–thaw cycles were carried out on four groups of samples soaked in sulfuric acid solution, sodium hydroxide solution, sodium chloride solution and pure water, respectively. Further, NMR tests were performed on the samples and the porosity change of samples,  $T_2$  distribution and nuclear magnetic resonance images were analyzed. Results show that: (1) chemical environments have significant effects on the freezing–thawing damage, and the porosity increases linearly with increasing number of freeze–thaw cycles. (2) Under the frost-heaving force and ionic reactions, the  $T_2$  spectrum will successively shift towards the left and then to the right with increasing number of freeze–thaw cycles. Micropores will constantly appear, and small pores will dynamically expand into macropores. (3) With increasing number of freeze–thaw cycles, the areas of light spots in NMR images will increase gradually, which means that the damage degree is aggravated with continuous development of internal pores. (4) The samples soaked in sodium hydroxide solution and sodium chloride solution are damaged more seriously than those soaked in sulfuric acid solution and pure water. By analyzing and comparing the NMR characteristics of rock under the coupled effects of chemical environments and

freeze–thaw cycles, more reliable test data will be available to study the damage mechanism of rock.

**Keywords** Chemical environments · Freeze–thaw cycles · Porosity · Rock damage ·  $T_2$  distribution · NMR images

## Introduction

With high development of the economy, soil and mineral resources in cold regions are increasingly exploited by humans. Studying the characteristics of rocks in cold regions under freeze–thaw cycles plays a key role in the field of road, civil and mining engineering.

Many efforts have been made to study the damage mechanism of rocks in cold regions. Most of them were related to the analysis of the properties of rock, such as physical and mechanical properties, porosity, pore size distribution and water absorption. Hori and Morihiro (1998) studied water freezing and moving in micropores by using a micromechanical model, and then predicted the deterioration degree of rock based on these microscopic processes. By using split Hopkinson pressure bar (SHPB) tests and nuclear magnetic resonance (NMR) technology, Del Río et al. (2005) carried out 56 freeze–thaw cycles on different types of granites with the temperature ranging from  $-12$  to  $20$  °C, and measured the ultrasonic velocity after each cycle. After freeze–thaw cycles, the number of pores, including micropores, was found to increase significantly. Sondergeld and Rai (2007) analyzed the physical parameters, including resistivity, compressional, and shear velocities, of Berea sandstone at cyclic temperature and elevated pressures. Yavuz (2011) performed ten freeze–thaw cycles and 50 thermal shock cycles on andesites, and found that the velocity of P wave, compressive

✉ Qiaoli Wang  
Qiaoli@csu.edu.cn

<sup>1</sup> School of Resource and Safety Engineering, Central South University, Changsha 410083, Hunan, China

<sup>2</sup> Mineral Resources Ministry of Aluminum Corporation of China, Beijing 100082, China

strength and hardness all decreased, while the porosity and water absorption increased. After exposing the rocks from cold regions to the freeze–thaw environments, Bayram (2012) investigated the loss of rock strength, and established the forecasting equation of uniaxial compressive strength for specific limestones. Liu et al. (2012) carried out freeze–thaw cycles on granites and andesites. After repeated freeze–thaw cycles, fine cracks and negative Poisson's ratio were observed. Martínez-Martínez et al. (2013) performed 100 freeze–thaw cycles on 102 carbonate rocks, and then analyzed the change of ultrasonic velocity attenuation, strength loss and porosity. With extensive tests, Fener and İnce (2015) studied the effects of the number of freeze–thaw cycles on basic physical and mechanical properties of the andesitic rocks. By incorporating the freeze–thaw correction coefficient into the expression of rock mass effect, Luo et al. (2015) analyzed the effects of freeze–thaw on the determination of parameters of slope rock mass in cold regions.

In addition to physical and mechanical properties, the chemical erosion of rocks also has been analyzed by a series of methods. Feucht and Logan (1990) evaluated the effect of chemical solutions (NaCl, CaCl<sub>2</sub> and Na<sub>2</sub>SO<sub>4</sub> solutions) on the frictional properties of quartz-rich sandstones by carrying out triaxial compression tests at varying ionic strengths and pH values. Karfakis and Akram (1993) studied the chemically activated fracturing mechanism of three types of rocks in five environments by using fracture mechanics techniques, and then formulated a possible intrinsic mechanism to modify the rock properties in chemical solutions. Feng et al. (2001) monitored the complete crack generation process of granites that were exposed to the air, NaCl, CaCl<sub>2</sub>, and NaHCO<sub>3</sub> solutions, and then compared the general character of the load–displacement curves and the ultimate compressive strength to study the effects of ionic concentrations and pH values on the fracturing behavior of samples. Zheng et al. (2015) performed triaxial compression and seepage–creep experiments to study the influence of water–chemical environments (CO<sub>2</sub>–NaCl solution) on the mechanical, hydraulic and chemical properties of quartz–feldspar–detritus sandstone.

Nuclear magnetic resonance (NMR) technology, which is a non-destructive spectroscopic testing technique, has been widely used to analyze the internal structure of rocks. The NMR equipment first transmits a radio frequency pulse with a certain frequency to rocks exposed to a magnetic field. Then, the nuclei <sup>1</sup>H in pore fluids will resonate with a radio frequency pulse, and absorb energy of the radio frequency pulse. After expiration of the radio frequency pulse, the absorbed energy will be further released. Finally, special dedicated coils can be used to detect the process of releasing energy, i.e., the NMR signal. The NMR signal

will differ in different size of pores, and then this difference can be used to describe the internal structure of rocks. For example, the rock porosity can be accurately obtained by detecting nuclei <sup>1</sup>H in pore fluids. Nowadays, several related studies are currently available in the literature. In the earlier studies, NMR technology was used to measure the porosity, movable fluid and permeability (Timur 1969) to determine pore size distribution (Howard and Kenyon 1992) or to measure other internal properties of rocks. Studies showed that compared with conventional technologies, NMR, as a nondestructive technology, has obvious advantages in terms of measurement of rock internal structure (Timur 1969), and it has powerful abilities to measure reservoir properties in a continuous log (Kenyon et al. 1995). In recent years, the NMR was used to predict permeability of sandstones based on the similarity between fluid movement and current flow in the pore space (Weller et al. 2010), to study the porosity changes associated with strength degradation (Shang et al. 2015), and to analyze the microscopic damage and dynamic mechanical properties of rocks subjected to recurrent freeze–thaw cycles (Zhou et al. 2015). In conclusion, to investigate the internal structure of rocks, NMR technology is a powerful tool.

Through the above analysis, it can be found that although the effects of both freeze–thaw cycle and chemical environment on rock damage have gotten more attention in the last decade, only most of the existing studies only take a single factor into consideration. However, in the real world, the effects of these two factors on rock damage may exist at the same time. From our case study, for example, samples were collected from Qinghai Province in China, where there is significant difference between temperatures during day and night, and saline soil is widely distributed. The saline soil can be mainly divided into three types: chlorine saline soil, sulfate saline soil, and carbonate saline soil, according to the properties of salt. These special soils will cause serious chemical corrosion to surrounding rocks at the same time as freeze–thaw cycles induced by sharp temperature difference. In consideration of this, different from the existing strategy which only considers a single factor, in this paper we studied the coupled effects of chemical environments and freeze–thaw cycles on the damage of red sandstones using NMR technology.

## Materials and methods

### Materials preparation

In this section, we introduce the experimental instruments, samples, and solutions used in this study.

The experimental instruments mainly include: TDS-300 concrete freeze–thaw test machine, AniMR-150 NMR imaging system (shown in Fig. 1), PL4002 electronic balance with precision of  $\pm 0.01$  g, Puxicoo P4-036 pocket waterproof pH test with precision of 0.01 pH, vernier, blowing dry box, and chemical experiment glassware.

The experimental samples, red sandstones, were collected from the subgrade of a road engineering in Qinghai Province, China. These sandstones were processed into samples with diameter of  $50 \pm 1$  mm, length of  $30 \pm 1$  mm, and flat ends. The average water absorption, saturated water ratio, and saturated water coefficient of these samples were measured as 1.65, 1.74, and 0.95 %, respectively. In the experiments, these samples were divided into four groups (labeled as C, D, E and F), and each group consisted of three samples (labeled as 7, 8, and 9), shown in Fig. 2. The physical parameters of the samples are shown in Table 1 (columns 2–5).

Four solutions were prepared in our experiments, including sulfuric acid solution (concentration of 1 % and initial pH value of 1.5), sodium hydroxide solution

(concentration of 1 % and initial pH value of 12.5), sodium chloride solution (concentration of 4 %) and pure water. The first three solutions were used to simulate the acid corrosion, alkaline corrosion, chloride corrosion in the real world, and the last one was used as a reference. The samples from groups C, D, E and F were soaked in sulfuric acid solution, sodium hydroxide solution, sodium chloride solution and pure water, respectively. The saturated weight of these samples is shown in Table 1.

### Experimental procedure

The pore is one of the microscopic characteristics of rocks. It plays an important role in studying the microscopic characteristics of freeze–thaw damage of rocks in complex chemical environments. Indeed, the meticulous measurement of pore size is a challenging task for NMR technology. On one hand, NMR technology can only detect the sign of fluid in rock pores, rather than that of rock framework. So, if the pores are not fully filled with fluid, the actual pore size can hardly be measured. On the other hand, pores are usually distributed in rocks with complex shapes, nonuniform size, inhomogeneous density and mixed connectivity. Thus, multiple measures based on NMR technology should be combined to comprehensively analyze the pore characteristic. In this study, all samples were saturated with their corresponding solutions, so that measurements based on NMR technology could reflect actual pore size. In addition, to describe the pore characteristic as comprehensive as desired, three measures of porosity,  $T_2$  distribution and NMR images were analyzed by using NMR technology, and more other measures will be tried in the future study. The specific experimental procedure is described as follows.

First, the samples in groups C, D, E and F were soaked in sulfuric acid solution, sodium hydroxide solution, sodium chloride solution and pure water, respectively. All of these samples were soaked for 48 h in order to observe better results in the following tests. Then the freeze–thaw test was conducted on all the saturated samples. During each cycle of freeze and thaw, the samples were frozen at  $-20$  °C for 8 h, and then thawed at  $20$  °C for another 8 h. In order to determine when the freeze–thaw cycle should be terminated, Brazilian split test was conducted to measure the tensile loss of samples. It turned out that after 30 freeze–thaw cycles, the samples in groups C, D, E and F were seriously damaged with average tensile losses of 22.4, 55.9, 42.2 and 12.8 %, respectively. In light of this, in this study, the freeze–thaw cycle was repeated 30 times in total. Before carrying out freeze–thaw tests and after every ten cycles, the following operations were performed.

The sulfuric acid and sodium chloride were added into their related solutions to control the pH value around the



**Fig. 1** AniMR-150 NMR imaging system



**Fig. 2** Experimental samples

**Table 1** Physical parameters of samples

Soaking solution	Samples	Diameter (cm)	Height (cm)	Initial weight (g)	Saturated weight (g)	Weight (g)			Weight increment (%)		
						10	20	30	10	20	30
H <sub>2</sub> SO <sub>4</sub>	C7	4.962	3.006	142.34	144.25	144.54	143.81	143.44	0.20	-0.51	-0.26
	C8	4.954	2.972	140.54	142.40	142.60	141.59	140.88	0.14	-0.71	-0.50
	C9	4.966	2.996	140.95	142.90	143.09	142.11	141.44	0.13	-0.68	-0.47
	Average	4.96	2.99	141.28	143.18	143.41	142.50	141.92	0.16	-0.63	-0.41
NaOH	D7	4.960	3.006	142.32	144.62	145.37	139.85	128.55	0.52	-3.80	-8.08
	D8	4.962	2.990	141.30	143.57	144.42	142.80	135.30	0.59	-1.12	-5.25
	D9	4.960	3.012	142.18	144.47	145.16	143.92	137.60	0.48	-0.85	-4.39
	Average	4.96	3.00	141.93	144.22	144.98	142.19	133.82	0.53	-1.92	-5.89
NaCl	E7	4.958	2.948	140.18	142.31	143.22	141.26	134.38	0.64	-1.37	-4.87
	E8	4.956	2.976	141.98	144.06	145.01	145.34	142.34	0.66	0.23	-2.06
	E9	4.958	2.960	139.97	142.00	142.89	140.10	133.31	0.63	-1.95	-4.85
	Average	4.96	2.96	140.71	142.79	143.71	142.23	136.68	0.64	-1.03	-3.90
Water	F7	4.962	2.998	141.80	143.99	144.36	144.08	144.13	0.26	-0.19	0.03
	F8	4.960	2.972	141.35	143.57	143.90	143.62	143.74	0.23	-0.19	0.08
	F9	4.960	2.976	141.51	143.79	143.94	143.81	143.95	0.10	-0.09	0.10
	Average	4.96	2.98	141.55	143.78	144.07	143.84	143.94	0.20	-0.16	0.07

initial level (1.5–2.5 and 11.5–12.5). By this means, we could ensure that the samples were exposed to stable chemical environments during the whole procedure. Then the four groups of samples were put back into their related solutions until they were saturated. Furthermore, NMR test was performed to measure the porosity and  $T_2$  distribution of the saturated samples by using the AniMR-150 NMR imaging analysis system. Finally, an NMR imaging test was conducted on the samples to obtain their two-dimensional cross-section images.

## Experimental results and analysis

In this section, the porosity,  $T_2$  distribution and NMR images are analyzed to study the coupled effect of chemical environments and freeze–thaw cycles on the rock damage, and then the damage evolution law is explained by discussing the ionic reactions and freeze–thaw action that occurred in the experiments.

### Analysis of porosity

Porosity refers to the fraction of void space in a material. It can quantitatively describe the change of pore structure of rocks. In this paper, the porosity was measured by using the AniMR-150 NMR imaging system. In Fig. 3, the relationship between the average porosity of samples in each group and the number of freeze–thaw cycles is shown.

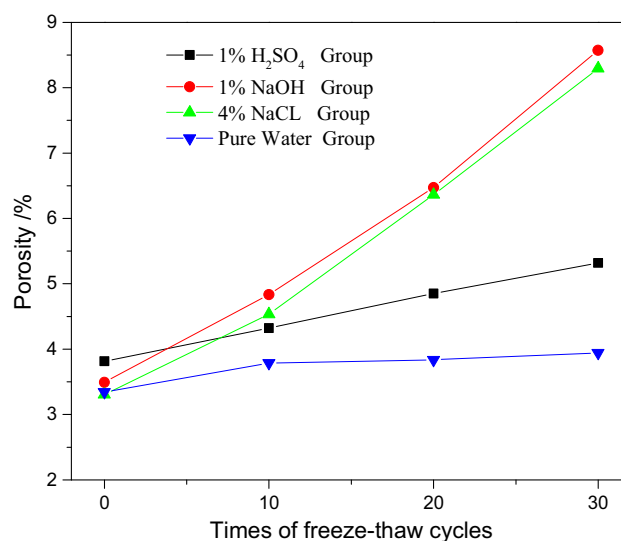


**Fig. 3** Porosity variation under the coupled effects of chemical environments and freeze–thaw cycles

From a general view of Fig. 3, one can see that the average porosity increases linearly with increase of the number of freeze–thaw cycles. Thus, it can be concluded that the damage rate of the pore structure of rocks is stable. In addition, the average porosity of samples in group F increases slowly with the increase of freeze–thaw cycles numbers, and after ten freeze–thaw cycles, it maintains a slower growth rate. The average porosity of samples in groups C, D and E increases faster than that in group F, and

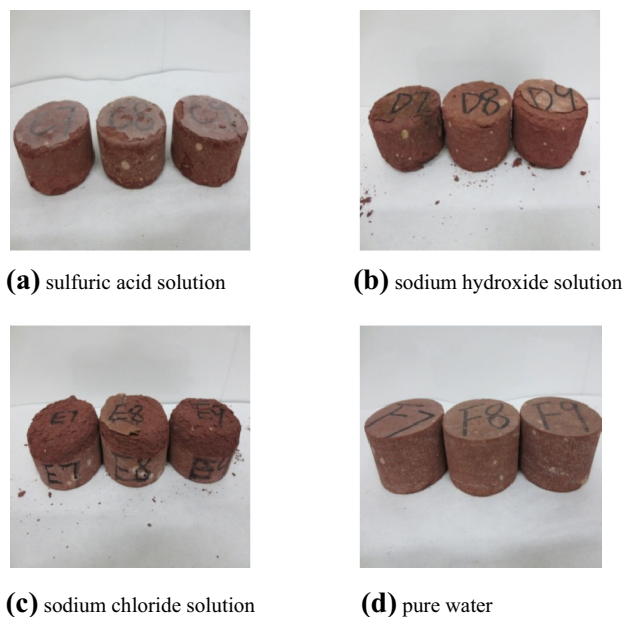


**Fig. 4** Samples after 30 freeze–thaw cycles in different solutions

the samples in groups D and E show the highest growth rate of the average porosity. In Table 1 (column 7–12) and Fig. 4, the changes of weight and appearance of samples after freeze–thaw cycles are shown. Similar phenomena can be found in that the samples in groups D and E show the maximal changes of weight, followed by those in group C, and macroscopic failure is observed in groups D and E, shown as peeling and fracture. One can also see that with the increasing freeze–thaw times, the weight of samples in chemical solution groups (C, D, and E) and the pure water group (F) has different variation tendencies. We argue that the three factors of solution absorption, freeze–thaw cycle and chemical erosion can lead to weight changes of the samples. For the pure water group, during the earlier period, solution absorption has a more significant effect, so the weight of samples increases; during the middle period, the freeze–thaw cycle gradually plays a leading role, so the weight of samples decreases; and during the later period, more and larger pores appear due to the freeze–thaw cycle, and then more water is absorbed into the samples, so the weight of the samples increases again. For the chemical solution groups, during the earlier period, the weight of the samples increases due to reasons similar to the above analysis; while during the middle and later period, more rocks fall down from the samples because of continuous chemical erosion, so decreased weight of the samples is observed. Based on the phenomena described above, one can see that compared with the pure water, the sulfuric acid solution, sodium hydroxide solution and sodium chloride solution can accelerate the freeze–thaw damage of rocks, and the latter two have the strongest influence. Thus, it can

be concluded that chemical environments have significant effects on the freeze–thaw damage of rocks.

### Analysis of $T_2$ distribution

The transverse relaxation time  $T_2$  of pore fluid is related to the size of pores in rocks, and the relaxation time is proportional to the size of pores (Mohnke 2014). The peak value and area of  $T_2$  distribution represent the concentration degree and amount of pores of different size. Thus,  $T_2$  distribution can be used to analyze the development and extension of pores in rocks, and accurately identify the spreading trend of rock damage. In the following, the  $T_2$  distributions of samples labeled by seven and nine in each group, are analyzed.

In Fig. 5, the  $T_2$  distributions of samples, labeled by seven in each group, are shown. It can be found that after each freeze–thaw cycle, the porosity and pore size of samples in groups C, D and E are greater than those in group F. This is ascribed to the ionic reaction between mineral composition and chemical solution. In general, the first  $T_2$  spectrum peak of each sample in each figure has the largest area. It means that most of the pores in samples are micropores. One can also see that the first  $T_2$  spectrum peaks of samples in groups C, D and E shift towards the right of that in group F, and the area of these peaks increases. This means that compared with the samples soaked in pure water, some micropores in samples, soaked in chemical solution, become larger, and new pores are generated in these samples. In addition, the last  $T_2$  spectrum peaks of samples in groups D and E shift towards the right of that in group F, and the area of these peaks increases significantly. This means that compared to the samples soaked in pure water, the amount of macropores in samples soaked in sodium hydroxide and sodium chloride solution increases, and the samples are seriously damaged. However, the area of the last  $T_2$  spectrum peak of samples in group C is a bit larger than that in group F, which means that the samples soaked in sulfuric acid solution are slightly damaged.

From Fig. 6a–d, one can see that with increasing number of freeze–thaw cycles, the first  $T_2$  spectrum peak shifts irregularly to the left or right, and the peak value fluctuates too, because there are not only new micropores generated, but also some pores extending to larger pores during the freeze–thaw cycles. However, the amount of new micropores generated and pores extending to larger pores cannot be quantitatively measured. Thus, the movements of the first  $T_2$  spectrum peak are irregular. It should be noted that the  $T_2$  spectrum peak of sample in group E changes significantly. It can probably be ascribed to the high concentration of the sodium chloride solution.

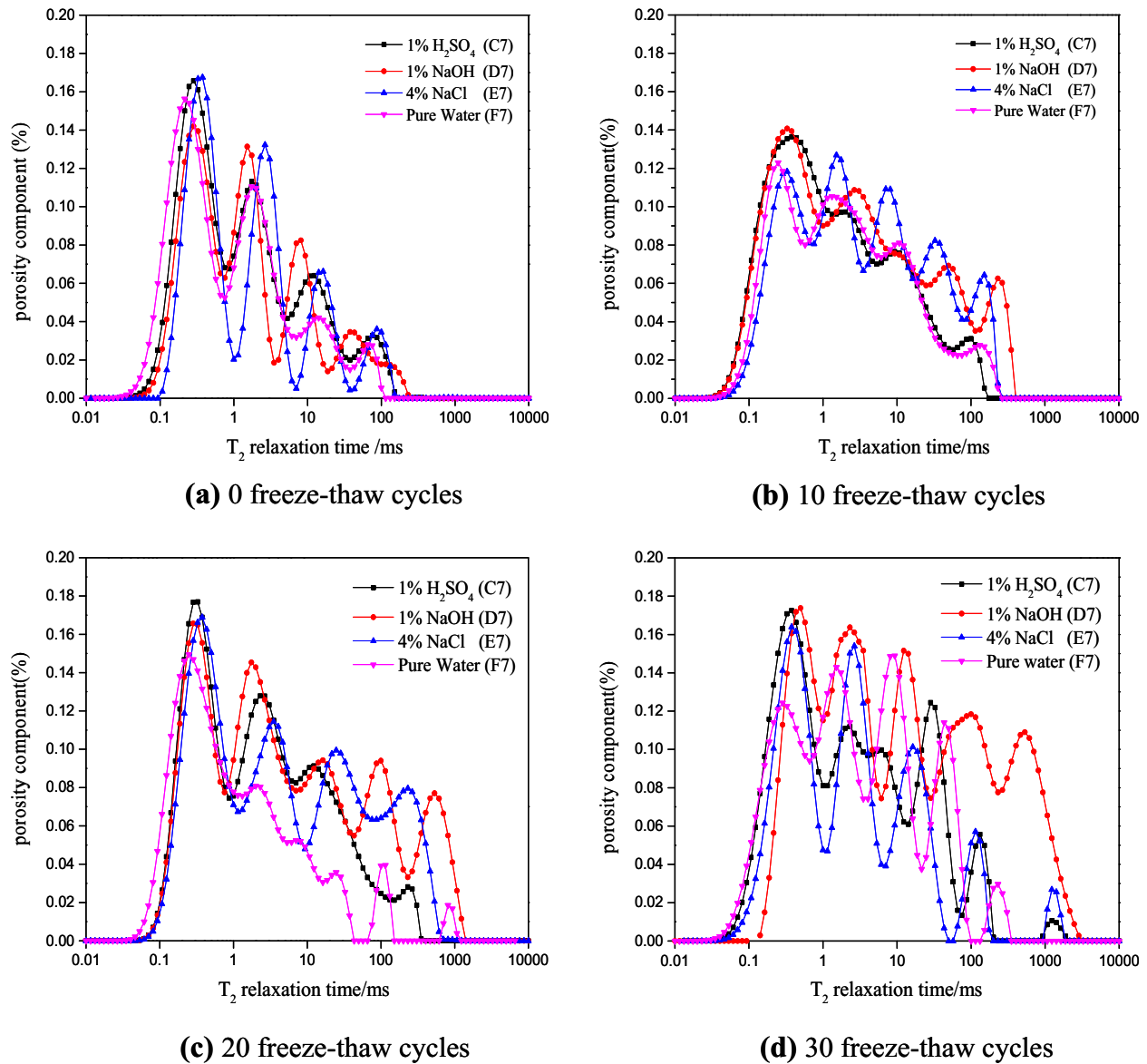


**Fig. 5**  $T_2$  distribution of samples, labeled by seven, soaked in different solutions experienced the same numbers of freeze–thaw cycles

### Analysis of NMR images

The attenuation characteristics of energy released by NMR differ in different compositions of rock. Thus, the locations and distribution of different compositions can be detected based on the difference of attenuation signal. As a result, the microstructure characteristics of rock can be discovered. In this study, after the freeze–thaw cycles, two-dimensional cross-section images of samples were obtained. The locations of fluid within rocks are shown as light spots in the NMR images, and the fluid content of samples is reflected by the brightness of light spots. The brighter and larger the light spots are, the higher the fluid content is, which means that the more and larger the pores are.

Considering the similarity of images of samples in the same group, only the NMR images of samples labeled by nine in each group are analyzed in the following.

The NMR images of C9 after different numbers of freeze–thaw cycles are shown in Fig. 7. One can see that the development of pores was from outside to inside. With increasing number of freeze–thaw cycles, the amount and area of light spots increased significantly. This means that the amount and size of pores within sample C9 increased significantly. Before freeze–thaw cycles, the NMR image is dark, but the light spots are uniformly distributed over the image. This indicates that the size of pores was small, but the distribution of pores was uniform. After ten freeze–thaw cycles, the amount of light spots in the surrounding

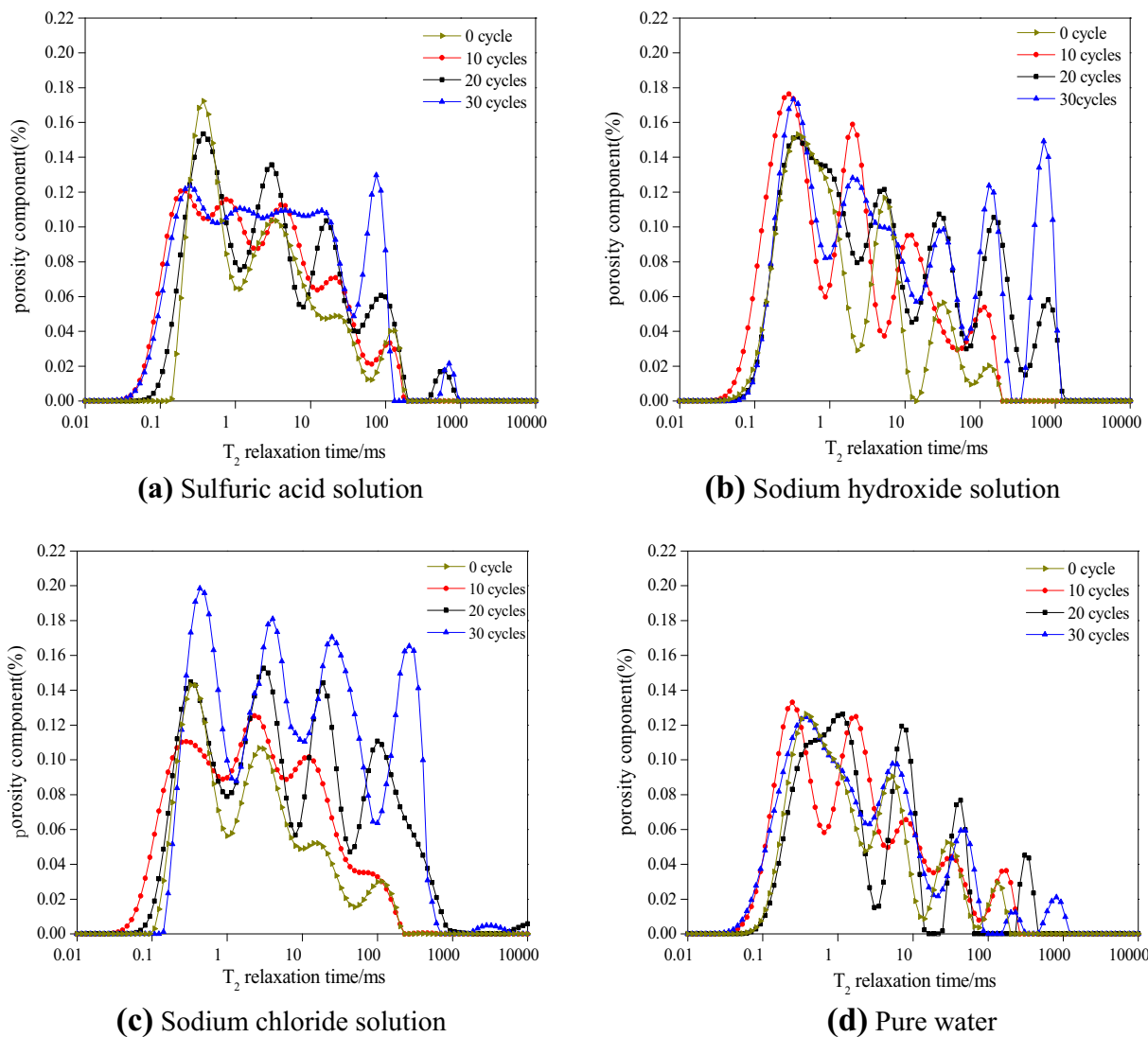
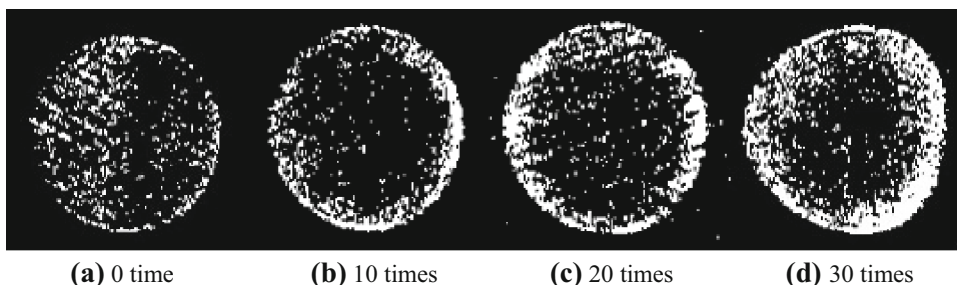


**Fig. 6** T<sub>2</sub> distribution of samples, labeled by nine, soaked in same the solutions experienced different numbers of freeze–thaw cycles

**Fig. 7** NMR images of C9 after different numbers of freeze–thaw cycles



area increased, which means that new pores appeared on the surface of this sample. After 20 freeze–thaw cycles, the amount and area of external light spots further increase, and the amount of internal light spots also increases. This means that the external small pores were extended to larger ones, and new pores were gradually developed within this

sample. After 30 freeze–thaw cycles, the external light spots expand to light areas, and the internal light spots become larger and brighter, meaning that the surface of this sample was surrounded with pore solution, and a part of this sample fell off. What’s more, a lot of pores were distributed within this sample.

**Fig. 8** NMR images of D9 after different numbers of freeze–thaw cycles

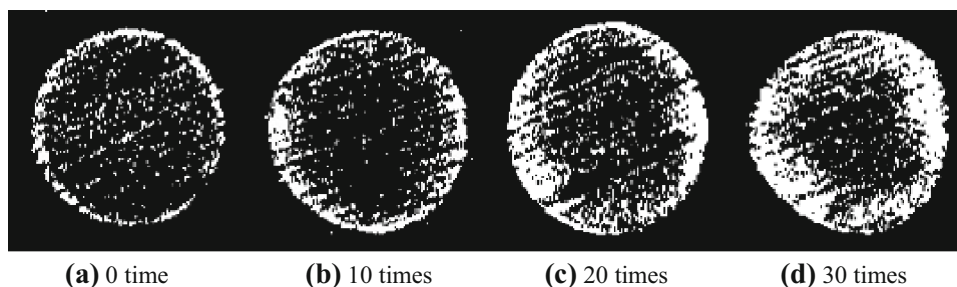
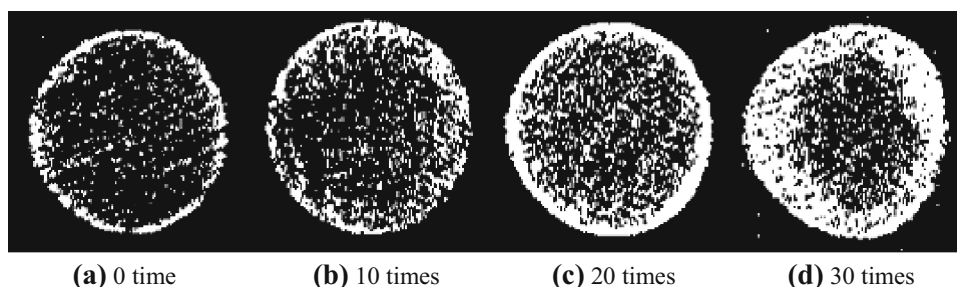


**Fig. 9** NMR images of E9 after different numbers of freeze–thaw cycles



As in the NMR images of sample D9 shown in Fig. 8, the light spots first connect with each other to form larger light areas in the outer layer, and then many new lights spots are developed within this sample. After 30 freeze–thaw cycles, the outer layer of this sample was obviously changed. The peeling of external rocks is ascribed to the freeze–thaw cycles and ionic reaction. In addition, almost all the external light spots are entirely connected with each other, and a big mass of large light areas is formed. This means that after repeated freeze–thaw cycles, the sample soaked in sodium hydroxide solution was seriously damaged on the surface, and a lot of secondary pores had developed.

In Fig. 9, the NMR images of sample E9 are shown. It can be found that similar to the development of pores in samples C9 and D9, the pores in sample E9 were developed from outside to inside. But, during the whole process of freeze–thaw tests, the NMR images are brighter, and more light spots are distributed over the images with more uniform densities. This means that the pores in this sample contained more solution, and they were distributed more uniformly. Thus, one can conclude that the sample soaked in sodium chloride solution will be damaged more seriously after the freeze–thaw cycles.

Finally, the NMR images of sample F9, which is soaked in pure water, are presented in Fig. 10. One can see that compared with images of samples in other groups, the light spots are distributed more uniformly with less amount, and the brightness and concentration degree of the lights spots are lower. This means that the pores in samples soaked in pure water had more even distribution and lower-level development, and no larger pores were formed.

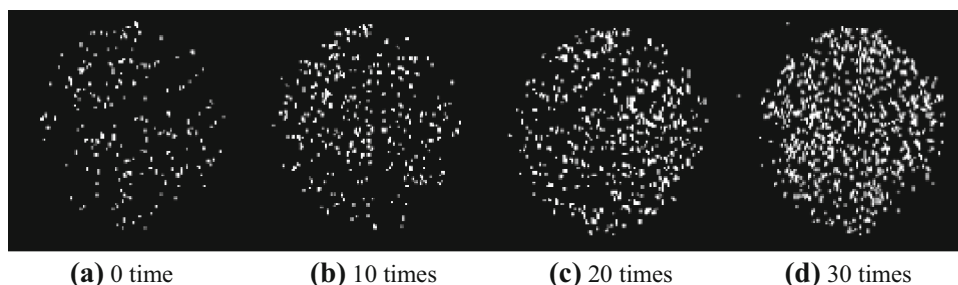
From the above analysis of NMR images, it can be found that the freeze–thaw damage of group D and E is the most serious, followed by group C, and the freeze–thaw damage of group F is the slightest. Thus, we can conclude that under the freeze–thaw environments, the effects of alkali and salt on the damage of rock are significant, and the effects of acid are less, but also cannot be ignored.

#### Investigation into the damage mechanism of rocks under the coupled effects of chemical environments and freeze–thaw cycles

Red sandstone is mainly composed of kaolinite, montmorillonite, hydromica, potassium feldspar, and cement (feruginous, calcareous, and siliceous), and is a porous material with non-uniform small pores. The initial average porosity of the samples used in this study was measured as 3.3 %. Chemical solutions, including hydrogen ion ( $H^+$ ), hydroxyl ion ( $OH^-$ ) and chloride ion ( $Cl^-$ ), can easily permeate through the large number of micropores existing on the surface and react with the minerals on the surface of samples. The connection of rock particles will be destroyed by the reaction. As a result, the surface of samples will become loose, and the amount of free particles will increase, which means that the porosity of samples will increase. The transfixion of pores will first occur on the surface of samples. Later, under the effect of freeze–thaw cycles, the chemical solutions will access the inside of samples and react with the internal mineral. It will lead to an increase of connected pores, and the development of micropores. As a result, the freeze–thaw damage of samples is accelerated.



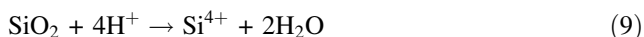
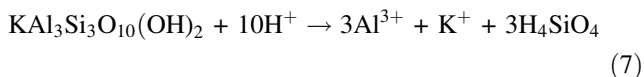
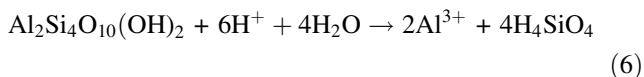
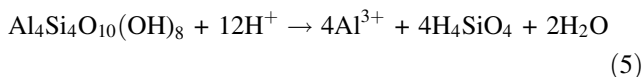
**Fig. 10** NMR imaging of E9 after different numbers of freeze–thaw cycles



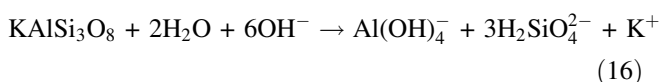
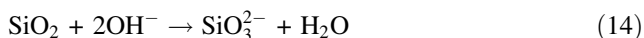
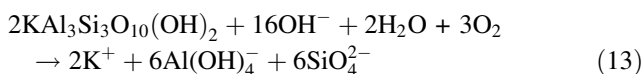
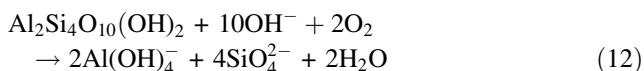
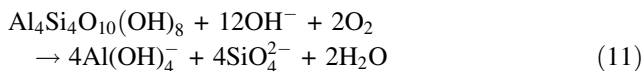
In the following, the chemical reactions between mineral of samples and solutions are described in detail. First, the reactions between red sandstone and pure water are listed in Eqs. (1)–(4).



Second, except for Eqs. (1)–(4), the main chemical reactions between red sandstone and sulfuric acid solution are shown as follows:



Third, except for Eqs. (1)–(4), the following chemical reactions mainly happen between red sandstone and sodium hydroxide solution.



Fourth, when the red sandstone is soaked in sodium chloride solution, the  $\text{O}_2^-$  of  $\text{Al}_2\text{O}_3$  will be replaced by the  $\text{Cl}^-$ , which is a living anion, and  $\text{Al}^{3+}$  will be combined with the  $\text{Cl}^-$  to form a complex ion. Consequently, a soluble chloride will be generated, and many etch pits will appear on the red sandstone. Meanwhile, the complex ion will also cut off the contact between  $\text{Al}^{3+}$  and  $\text{O}_2^-$ . Then, the  $\text{O}_2^-$  will react with  $\text{H}_2\text{O}$  to form  $\text{OH}^-$ , and the  $\text{OH}^-$  will further react with  $\text{Al}_2\text{O}_3$  under the alkaline environments. Thus, the corrosion of red sandstone will be accelerated. Similar chemical reactions will happen between  $\text{Fe}_2\text{O}_3$  and sodium chloride solution.

In addition, the damage of rocks under chemical environments is closely related to the temperature and number of freeze–thaw cycles. As the temperature decreases, the pore solution will freeze. Then, the volume of pore solution will expand, which means that a greater frost-heaving force will form between mineral particles and rock pores. Finally, rock damage will be aggravated. As the temperature increases, the frozen pore solution within rocks will melt. Then the frozen stress will be released, which means that the solution will migrate to other places. It will also contribute to rock damage. What's more, with the increasing number of freeze–thaw cycles, the rock structure will continually be destroyed by the cyclic effects of frost-heaving force and solution migration, which leads to an increase in the development of pores. Thus, it will further be helpful for samples to be exposed to the chemical solutions, and then the weak connection of rock particles will be further weakened. When the frost-heaving force reaches the ultimate tensile strength of the pore wall, the internal pores will become larger, and the external pores will be connected with each other. As we can see from the appearance, the outer layers of the rock start peeling off. Finally, the structure of the samples is destroyed.

In conclusion, together, chemical solutions and freeze–thaw cycles destroy rocks and help each other forward. Based on the damage mechanism analyzed above, we can easily understand why the samples are damaged from outside to inside, and why the freeze–thaw damage of samples soaked in chemical solutions is more serious than that of samples soaked in pure water.

## Conclusions

To provide more useful insights into rock damage in natural environments, we studied the coupled effects of chemical environments and freeze–thaw cycles in this paper. Based on critical analysis of porosity,  $T_2$  distribution and NMR images by using NMR technique, the following conclusions can be drawn:

1. According to the changing rule of porosity observed after the freeze–thaw cycles, chemical environments have great effects on the rock samples. With an increasing number of freeze–thaw cycles, the mass of samples except those soaked in pure water decreased significantly, and the surface of these samples deteriorated and spalled to different degrees.
2. After the freeze–thaw cycles, the  $T_2$  distribution and pore structure of red sandstone changed significantly. In the initial stage of freeze–thaw cycles, new secondary small pores were generated in the red sandstone. As a result, the amount of small pores absolutely increased. With an increasing number of freeze–thaw cycles, the small pores gradually extended to macropores. In addition, chemical solutions aggravate rock damage. The influences of sodium hydroxide and sodium chloride solutions are the most significant, and the influence of sulfuric acid solution is relatively weak. The whole process, including generation, expansion and collapse of the interior pores, was dynamic. Finally, under the coupled effect of chemical environments and freeze–thaw cycles, the destruction of samples could be observed at the macro level, due to the transfixion of macropores.
3. According to the internal and external pore distribution observed from the results of NMR imaging, it can be concluded that chemical solutions have great effects on the microstructure of rocks. One can also see that the samples are gradually destroyed from outside to inside, and the outer damage will further lead to the transfixion of pores and peeling of external rocks.

**Acknowledgments** The authors are grateful to anonymous reviewers whose constructive comments were helpful for this paper's revision. The support from National Natural Science Foundation of China (Grant No. 51474252), National Key Scientific Instrument and Equipment Development Project of China (Grant No. 2013YQ17046310), Innovation Driven Plan of Central South University (Grant No. 2015CX005), and Postgraduate Research and Innovation Foundation of Central South University (Grant No. 2015zts261) is highly appreciated.

## References

Bayram F (2012) Predicting mechanical strength loss of natural stones after freeze–thaw in cold regions. *Cold Reg Sci Technol* 83–84(2012):98–102. doi:[10.1016/j.coldregions.2012.07.003](https://doi.org/10.1016/j.coldregions.2012.07.003)

- Del Río LM, et al (2005) Ultrasonic study of alteration processes in granites caused by freezing and thawing. *IEEE Ultrason Symp* 415–418. doi:[10.1109/ULTSYM.2005.1602882](https://doi.org/10.1109/ULTSYM.2005.1602882)
- Fener M, İnce İ (2015) Effects of the freeze–thaw (FT) cycle on the andesitic rocks (Sille-Konya/Turkey) used in construction building. *J Afr Earth Sci* 109(2015):96–106. doi:[10.1016/j.jafrearsci.2015.05.006](https://doi.org/10.1016/j.jafrearsci.2015.05.006)
- Feng X, Chen S, Li S (2001) Effects of water chemistry on microcracking and compressive strength of granite. *Int J Rock Mech Min Sci* 38(4):557–568. doi:[10.1016/S1365-1609\(01\)00016-8](https://doi.org/10.1016/S1365-1609(01)00016-8)
- Feucht LJ, Logan JM (1990) Effects of chemically active solutions on shearing behavior of a sandstone. *Tectonophysics* 175(1):159–176. doi:[10.1016/0040-1951\(90\)90136-V](https://doi.org/10.1016/0040-1951(90)90136-V)
- Hori M, Morihiro H (1998) Micromechanical analysis on deterioration due to freezing and thawing in porous brittle materials. *Int J Eng Sci* 36(4):511–522. doi:[10.1016/S0020-7225\(97\)00080-3](https://doi.org/10.1016/S0020-7225(97)00080-3)
- Howard JJ, Kenyon WE (1992) Determination of pore size distribution in sedimentary rocks by proton nuclear magnetic resonance. *Mar Pet Geol* 9(2):139–145. doi:[10.1016/0264-8172\(92\)90086-T](https://doi.org/10.1016/0264-8172(92)90086-T)
- Karfakis MG, Akram M (1993) Effects of chemical solutions on rock fracturing. In: *International journal of rock mechanics and mining sciences & geomechanics abstracts*. Elsevier, Amsterdam, pp 1253–1259. doi:[10.1016/0148-9062\(93\)90104-L](https://doi.org/10.1016/0148-9062(93)90104-L)
- Kenyon B et al (1995) Nuclear magnetic resonance imaging—technology for the twenty-first century. *Oilfield Rev* 7(3):19–33
- Liu H et al (2012) Acoustic experimental study of two types of rock from the Tibetan Plateau under the condition of freeze–thaw cycles. *Sci Cold Arid Reg* 4(1):21–27. doi:[10.3724/SP.J.1226.2012.00021](https://doi.org/10.3724/SP.J.1226.2012.00021)
- Luo X et al (2015) Effects of freeze–thaw on the determination and application of parameters of slope rock mass in cold regions. *Cold Reg Sci Technol* 110(2015):32–37. doi:[10.1016/j.coldregions.2014.11.002](https://doi.org/10.1016/j.coldregions.2014.11.002)
- Martínez-Martínez J et al (2013) Non-linear decay of building stones during freeze–thaw weathering processes. *Constr Build Mater* 38:443–454. doi:[10.1016/j.conbuildmat.2012.07.059](https://doi.org/10.1016/j.conbuildmat.2012.07.059)
- Mohnke O (2014) Jointly deriving NMR surface relaxivity and pore size distributions by NMR relaxation experiments on partially desaturated rocks. *Water Resour Res* 50(6):5309–5321. doi:[10.1002/2014WR015282](https://doi.org/10.1002/2014WR015282)
- Shang J et al (2015) Porosity increment and strength degradation of low-porosity sedimentary rocks under different loading conditions. *Int J Rock Mech Min Sci* 75(2015):216–223. doi:[10.1016/j.ijrmms.2015.02.002](https://doi.org/10.1016/j.ijrmms.2015.02.002)
- Sondergeld CH, Rai CS (2007) Velocity and resistivity changes during freeze–thaw cycles in Berea sandstone. *Geophysics* 72(2):E99–E105. doi:[10.1190/1.2435198](https://doi.org/10.1190/1.2435198)
- Timur A (1969) Pulsed nuclear magnetic resonance studies of porosity, movable fluid, and permeability of sandstones. *J Pet Technol* 21(06):775–786. doi:[10.2118/2045-PA](https://doi.org/10.2118/2045-PA)
- Weller A, Nordsiek S, Debschütz W (2010) Estimating permeability of sandstone samples by nuclear magnetic resonance and spectral-induced polarization. *Geophysics* 75(6):E215–E226. doi:[10.1190/1.3507304](https://doi.org/10.1190/1.3507304)
- Yavuz H (2011) Effect of freeze–thaw and thermal shock weathering on the physical and mechanical properties of an andesite stone. *Bull Eng Geol Environ* 70(2):187–192. doi:[10.1007/s10064-010-0302-2](https://doi.org/10.1007/s10064-010-0302-2)
- Zheng H, Feng X, Pan P (2015) Experimental investigation of sandstone properties under CO<sub>2</sub>–NaCl solution–rock interactions. *Int J Greenh Gas Control* 37(2015):451–470. doi:[10.1016/j.ijggc.2015.04.005](https://doi.org/10.1016/j.ijggc.2015.04.005)
- Zhou KP et al (2015) Microscopic damage and dynamic mechanical properties of rock under freeze–thaw environment. *Trans Nonferr Met Soc China* 25(4):1254–1261. doi:[10.1016/S1003-6326\(15\)63723-2](https://doi.org/10.1016/S1003-6326(15)63723-2)